Article

Interactions of Co(II)- and Zn(II)porphyrin of 5,10,15,20-tetrakis(1-methyl-4-pyridinio)porphyrin with DNA in Aqueous Solution and Their Antimicrobial Activities

Nusrat Jahan Upoma, Nazmin Akter, Farhana Khanam Ferdousi, Md. Zakir Sultan, Shofiur Rahman, Abdullah Alodhayb, Khuloud A. Alibrahim, and Ahsan Habib*

ACCESS | Metrics & More | Article Recommendations

Co(II)- and [Zn(II)TMPyP]⁴⁺ → Microbial growth inhibition induced by metalloporphyrins
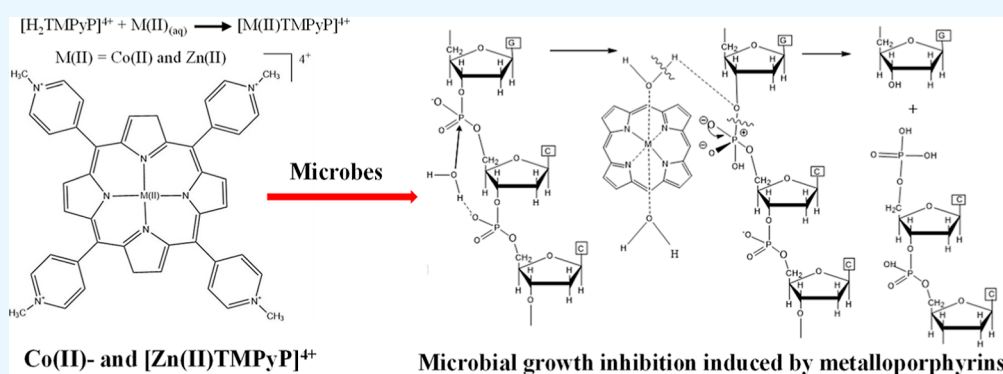
ABSTRACT: Antibiotics are frequently used to treat, prevent, or control bacterial infections, but in recent years, infections resistant to all known classes of conventional antibiotics have significantly grown. The development of novel, nontoxic, and nonincursive antimicrobial methods that work more quickly and efficiently than the present antibiotics is required to combat this growing public health issue. Here, Co(II) and Zn(II) derivatives of tetrakis(1-methylpyridinium-4yl)porphyrin $[H_2TMPyP]^{4+}$ as a tetra(ρ-toluenesulfonate) were synthesized and purified to investigate their interactions with DNA (pH 7.40, 25 °C) using UV−vis, fluorescence techniques, and antimicrobial activity. UV−vis results showed that $[H_2TMPyP]^{4+}$ had a high hypochromicity (∼64%) and a substantial bathochromic shift ($\Delta\lambda$, 14 nm), while $[Co(II)TMPyP]^{4+}$ and $[Zn(II)TMPyP]^{4+}$ showed little hypochromicity (∼37%) and a small bathochromic shift ($\Delta\lambda$, 3−6 nm). Results reveal that $[H_2TMPyP]^{4+}$ interacts with DNA via intercalation, while Co(II)- and $[Zn(II)TMPyP]^{4+}$ interact with DNA via outside self-stacking. Fluorescence results also confirmed the interaction of $[H_2TMPyP]^{4+}$ and the metalloporphyrins with DNA. Results of the antimicrobial activity assay revealed that the metalloporphyrins showed inhibitory effects on Gram-positive and Gram-negative bacteria and fungi, but that neither the counterions nor $[H_2TMPyP]^{4+}$ exhibited any inhibitory effects. Mechanism of antimicrobial activities of metalloporphyrins are discussed.

1. INTRODUCTION

Porphyrins are the most widespread organic molecules in nature and belong to a particular class of heterocyclic tetrapyrrolic organic molecules. From a structural perspective, porphyrins are made up of four pyrrolic units that are linked in a coplanar form by four methene bridges, providing the porphyrin molecule with a planar macrocyclic structure. They exhibit aromatic behavior due to their extended conjugated 18-electron system, and their small cavity size allows for the accommodation of large metal cations.[1,2] Porphyrins are necessary for living organisms because they play a role in a number of biological activities, including oxygen binding, electron transfer, biocatalysis, and photochemical pathways. In biological systems, metals are frequently bound to porphyrins to produce metalloporphyrins. For instance, iron binds to

porphyrin to generate hemoglobin, which, in mammals, is in charge of complex oxygen transport. However, magnesium binds to porphyrin to produce chlorophyll, which functions as a light-harvesting component in the photosynthesis process.[3,4] Synthetic porphyrins and metalloporphyrins have intriguing biological, photophysical, and photochemical features and hold great promise for the treatment of diseases,[5,6] biological
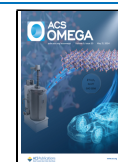
imaging,[7] industrial,[8] analytical,[9] photocatalytic,[10] nonlinear optics,[11] and molecular photovoltaics.[12,13]

Cationic porphyrins and their metal complexes have been found to offer certain advantages as model drugs and probes because they are water-soluble, have deep color, many of them fluoresce, offer simple signals for monitoring reactions, and can bind tightly to nucleic acids.[14-25] Thus, many attempts have been made to investigate how cationic porphyrins and their metalloderivatives interact with DNA.[16-20,22-25] The DNA binding mechanism is highly dependent on both the structure of the porphyrin molecules and the sequencing of the DNA strands.[16-20,22-25] Tetrakis(1-methylpyridinium-4-yl)-porphyrin, $[H_2TMPyP]^{4+}$, a planar free base porphyrin (Figure 1), and its metal complexes, such as Pt(II) and Pd(II), which lack axial ligands, intercalate with DNA to bind it, preferentially in the GC-rich regions of DNA strands.[16-20,22-25]
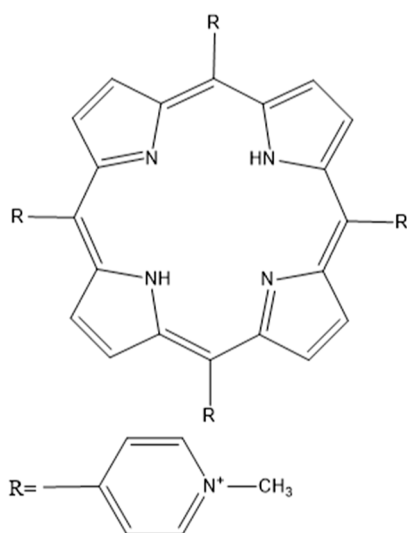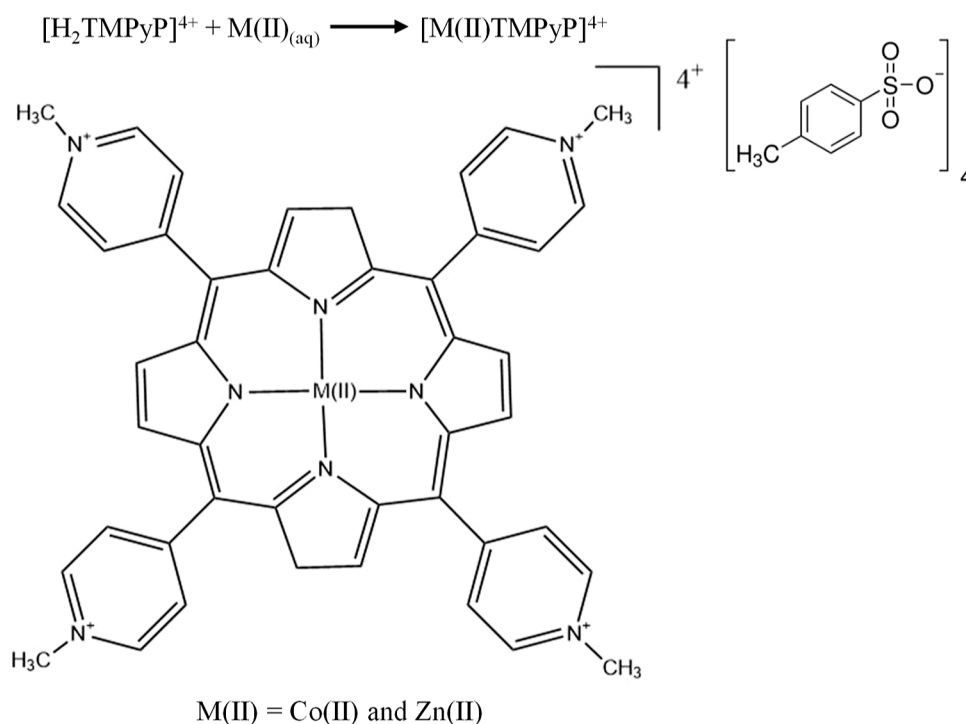

Figure 1. Structure of tetrakis(1-methylpyridinium-4-yl)porphyrin, $[H_2TMPyP]^{4+}$, a planar free base porphyrin.

The axial ligand-containing metalloporphyrins of complexes, such as Mn(III), Fe(III), Co(III) and Ru(II), preferentially bind to DNA in the AT-rich areas of DNA grooves through outside self-stacking.[16-18,20,22] In contrast, $[Au(III)TMPyP]^{5+}$ interacts with DNA through outside self-stacking and partial intercalation.[18] Additionally, the ratio of porphyrin to DNA and the ionic strength of the solution in which the interaction occurs have an impact on the binding modes.[18,20,22] The cationic porphyrins, such as $[H_2TMPyP]^{4+}$ and meso-5,10,15-tris(N-methyl-4-pyridiniumyl)-20-(4-alkylamidophenyl) porphyrins, intercalate into DNA, notably at GC-rich regions, at low porphyrin-to-DNA ratios and low ionic strengths.[26] The binding mode involves both intercalation at GC sites and groove binding, which primarily takes place at AT sites, if the porphyrin to DNA ratios and/or ionic strength are raised.[27,28] The porphyrin can bind externally to form long-range stacked structures on the outside of the nucleic acid at high ionic strengths. Similar to intercalating porphyrins, this interaction is marked by a red shift and a notable drop in the Soret band's intensity.[29] It is mentioned that intercalation requires only half of the porphyrin ring.

One of the biggest clinical challenges in the world has been the fast-increasing bacterial antibiotic resistance. Historically,

bacterial infections have been controlled, treated, or prevented with antibiotics. Resistance, however, has been a greater problem in recent years, particularly in hospitals. Inappropriate prescriptions of ineffective medications in the environment and the regular transmission of microorganisms around the world by travelers also pose serious problems.[30] Many epidemiological investigations have demonstrated that in the last 30 years, bacterial resistance to all known classes of conventional antibiotics has significantly grown, particularly in hospitals, rendering some regimens useless.[31,32] According to reports, for instance, methicillin-resistant *Staphylococcus aureus* type t002 isolates from hospitals in the United States significantly increased in 2013.[33,34] According to reports, the centers for disease control and prevention estimated that 10% of patients treated to American hospitals develop a hospital-acquired infection; many of these patients go on to pass away as a result of their diseases.[35] However, the situation is far worse in countries that are developing, where the infection rate is around 75%.[36-38] To combat the increasing number of resistant bacterial strains that have arisen in this century, however, the most recent developments in the search for new antibiotics fall short.[31] A nonincursive, nontoxic, and novel antimicrobial approach that acts faster and more efficiently than the available antibiotics must be developed in order to combat this rising public health issue.[39-41] Antibacterial photodynamic treatment (aPDT) is one of these techniques.[42] Many investigations have shown that aPDT is effective against conventionally resistant bacteria in clinical trials,[43] animal models,[44] and in vitro.[45] As an example, in vitro testing showed that aPDT effectively eliminated a clinical isolate of *Pseudomonas aeruginosa*, which is regarded as one of the most dangerous nosocomial bacteria.[46]

According to Tabata and co-workers, metalloporphyrins with axial ligands interact with DNA by outside self-stacking and show accelerated DNA cleavage in the presence of low concentrations of restriction enzyme, where the enzyme cannot cut the phosphodiester linkage of DNA molecules.[47-49] It is important to note that restriction enzymes are present in microorganisms, primarily in bacteria, and they serve to defend them from bacteriophages (e.g., viruses) that are attempting to invade. This system is mostly responsible for the destruction of undesired foreign DNA that enters cells as a result of infection. Thus, the metalloporphyrins having axial ligands could be suitable candidates as antibacterial agents because of the presence of restriction enzymes in microbes. Here, metalloporphyrins of Co(II) and Zn(II) with the free base porphyrin, $[H_2TMPyP]^{4+}$ (Figure 2), were prepared to investigate their interactions with DNA. We subsequently investigated the antimicrobial abilities of the metalloporphyrins. We report on the finding that metalloporphyrins with axial ligands inhibit bacterial growth at very low concentrations where the free base porphyrin, $[H_2TMPyP]^{4+}$, and other metalloporphyrins having no axial ligands do not exhibit antibacterial activities. The presence of a restriction enzyme in bacteria could play a vital role in cleaving the phosphodiester bonds of DNA molecules through the formation of hydrogen bonding between the hydrogen atom of water molecules and the oxygen atom of the phosphodiester bonds. Other studies, however, demonstrated that metalloporphyrins might also be used in photodynamic therapy (PDT) as antibacterial agents.[50-54] In a PDT system, light excites the porphyrins, which then generate free radicals, particularly reactive oxygen species, that cleave biomolecules, including DNA.

$$[H_2TMPyP]^{4+} + M(II)_{(aq)} \longrightarrow [M(II)TMPyP]^{4+}$$

M(II) = Co(II) and Zn(II)

Figure 2. Structures of metalloporphyrins of Co(II) and Zn(II) with $[H_2TMPyP]^{4+}$, $[Co(II)TMPyP]^{4+}$, and $[Zn(II)TMPyP]^{4+}$ with the counterion, tetra(p-toluenesulfonate).

2. EXPERIMENTAL SECTION

2.1. Chemicals and Reagents. 5,10,15,20-Tetrakis(1-methyl-4-pyridinio) porphyrin tetra(ρ-toluenesulfonate) $[H_2(TMPyP)]^{4+}$ was purchased from Sigma-Aldrich, USA. A stock solution of the free base porphyrin was prepared by using distilled water. The concentration of the stock solution of free base porphyrin was determined using a series of standard copper(II) solutions in a spectrophotometric titration (molar ratio approach). An explanation of the procedure has been given previously.[15,55] In short, a constant concentration of the free base porphyrin is used to titrate various concentrations of standard Cu(II) solutions. When a constant concentration of free base porphyrin is added, the absorbance of the Cu(II)porphyrin complex increases with increasing Cu(II) solution concentration, but it remains constant at the 1:1 molar ratios. The absorbance of each titration is plotted against the concentration of the Cu(II) solution. The concentration of the free base porphyrin is represented by the point on the x-axis where the absorbance remains constant. A 1:1 ratio of metal ions, such as Co(II) and Zn(II), and free base porphyrin solutions has been used for the formation of metalloporphyrins (Figure 2). Then the mixtures were purified by recrystallizing with $NaClO_4$ and running them through an anion exchange resin. The purity of the synthesized metalloporphyrins were confirmed by their absorption maxima (λ_{max}) using UV−vis spectra. The absorption maxima (λ_{max}) of $[Co(II)TMPyP]^{4+}$ and $[Zn(II)TMPyP]^{4+}$ were found to be 438 and 437 nm, respectively.[21,22,56−60] Salmon fish sperm DNA purchased from Sigma-Aldrich, USA was used to make a stock solution in distilled water, and the concentration of the base pairs was determined by monitoring the absorbance at λ_{max} = 260 nm using known molar extinction coefficient, ε_{260} = 1.32 × 10^4 M^{-1} cm^{-1}.[21,22] The stock solution of DNA was stored at −4 °C and incubated in a water bath at 37 °C for 1 h before

carrying out the experiments. Cobalt chloride, zinc chloride, sodium chloride, sodium nitrate, sodium hydroxide, and hydrochloric acid were purchased from Merck, Germany. 2-[4-(2-Hydroxyethyl)-1-piperazinyl]ethanesulfonic acid (HEPES) was purchased from Sigma-Aldrich, USA, and used as a buffer solution. All of the experiments were carried out under physiological conditions (pH = 7.4).

2.2. DNA-Porphyrin Interaction. UV−vis spectrophotometer (UV-1800, SHIMADZU, Japan) and fluorescence spectrophotometer (F-7000, HITACHI, Japan) were used to investigate the interaction between DNA and the free base porphyrin and its metalloderivatives. The progress of the interaction between DNA and porphyrins was monitored by observing the changes in the absorbance of the relevant metalloporphyrin upon the addition of DNA. For example, the absorbances for $[H_2TMPyP]^{4+}$, $[Co(II)TMPyP]^{4+}$, and $[Zn-(II)TMPyP]^{4+}$ have been measured at 422, 438, and 437 nm, respectively.

A fluorescence spectrophotometer (F-7000, Hitachi, Japan) was also employed to investigate the interactions of DNA with the porphyrins. The fluorescence spectra were recorded by setting the fluorescence excitation wavelength at 433, 448, and 449 nm for $[H_2TMPyP]^{4+}$, $[Co(II)TMPyP]^{4+}$, and $[Zn(II)-TMPyP]^{4+}$, respectively, because the isosbestic points of the binary system of free base porphyrin-DNA and metalloporphyrin-DNA were observed at those wavelengths. The wavelengths of emission were maintained at 550−800 nm.

2.3. Antimicrobial Activity. The novel synthesized $[Co(II)TMPyP]^{4+}$ and $[Zn(II)TMPyP]^{4+}$ complexes were screened against pathogenic bacteria and fungi using the disc diffusion method in order to investigate their in vitro antimicrobial activities. The screening was performed against five Gram-positive bacterial strains including *Bacillus cereus*, *Bacillus magaterium*, *Bacillus subtilis*, *S. aureus*, *Sarcina lutea*, and eight Gram-negative bacterial strains like *Escherichia coli*, *P.*

aeruginosa, *Salmonella paratyphi*, *Salmonella typhi*, *Shigella boydii*, *Shigella dysenteriae*, *Vibrio mimicus*, and *Vibrio parahemolyticus*. Antifungal studies were carried out in three fungal strains (filamentous), for example, *Saccharomyces cerevisiae*, *Candida albicans*, and *Aspergillus niger*. All the susceptible bacterial and fungal strains were collected as pure cultures from the State University of Bangladesh (SUB), Dhaka, Bangladesh. The microorganisms were American Type Culture Collection standard strains. Few of them were clinical isolated and some of them were isolated from the environment. None of them was isolated from human directly.

The bacterial and fungal stock cultures were primarily inoculated in nutrient medium, followed by incubation at 37 °C. Constituents of nutrient medium were bacto beef extract (0.3 g), bacto peptone (0.5 g), agar (1.5 g), distilled water (100 mL), and sodium chloride (0.8 g). The pH of the medium was adjusted to 7.2−7.6. Preinoculated bacterial and fungal suspensions were transferred from the subculture to the test tubes containing about 10 mL of melted and sterilized agar medium with the help of a sterilized transfer loop in an aseptic area, immediately transferred to the aseptically prepared Petri dishes, and allowed to dry at room temperature. About 10 μL of sample (13.5 μg) was directly allotted into the small wall made in the preinoculated Petri dish, as shown in Figure 3
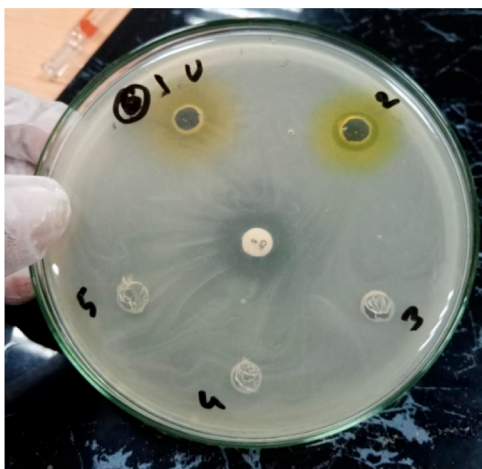
Figure 3. Test plate for the determination of the clear zone of inhibition.

(photograph was taken by one of the coauthors, Nusrat Jahan Upoma). Standard antibiotic used as a positive control in this investigation is ciprofloxacin (5 μg/disc). Blank run of counter metal ions and free base porphyrin was also carried out to find out if they have any antimicrobial activity at that concentration level. After introducing sample and standard, the Petri dishes were kept in a refrigerator at 4 °C for 24 h to ensure diffusion of the test materials and finally incubated at 37 ± 1 °C for 24 h. The diameter of the zone of inhibition was measured in millimeters to evaluate the antimicrobial activity of the test samples. The assay was carried out twice to avoid possible inaccuracy of this study.

3. RESULTS AND DISCUSSION

3.1. UV−Vis Spectral Analysis of the Interaction of DNA with [H$_2$TMPyP]$^{4+}$ and Its Metallocomplxes, Co(II)- and [Zn(II)-TMPyP]$^{4+}$, in Aqueous Solution. Figure 4a−c shows the change in the spectral pattern upon the successive

addition of DNA into [H$_2$TMPyP]$^{4+}$, [Co(II)TMPyP]$^{4+}$, and [Zn(II)TMPyP]$^{4+}$, respectively. As seen from Figure 4a, substantial hypochromicity (∼64%) and a large bathochromic shift ($\Delta\lambda$ = 14 nm) were observed upon the addition of DNA solution into the free base porphyrin. The concentration of DNA solution was maintained between 0 and 2.0 × 10^{-5} M base pairs.

However, [Co(II)TMPyP]$^{4+}$ and [Zn(II)TMPyP]$^{4+}$ showed a minimal hypochromicity and a small bathochromic shift upon the addition of DNA ranging from 0 to 2.4 × 10^{-4} M base pairs, and the values were found to be ∼37 and ∼38%, $\Delta\lambda$ = 3 and 6 nm, respectively (Figure 4a−c). These results suggested that the free base porphyrin interacts with DNA through intercalation and both the metalloporphyrins interacted with DNA through outside self-stacking with partial intercalation.[18,20,22,60−64] It makes sense that the bulkiness of the metalloporphyrins results from their axial ligands, water molecules, preventing them from intercalating into DNA grooves. On the other hand, free base porphyrins and/or metalloporphyrins without axial ligands interact with DNA through intercalation. Additionally, the interactions between DNA and the metalloporphyrins were investigated using fluorescence spectroscopy and are presented in the following section.

3.2. Fluorescence Spectral Analysis of the Interaction of DNA with [H$_2$TMPyP]$^{4+}$ and Its Metalloderivatives, [Co(II)TMPyP]$^{4+}$ and [Zn(II)TMPyP]$^{4+}$, in Aqueous Solution. The interactions of DNA with the free base porphyrins and its metalloderivatives of Co(II) and Zn(II) were also investigated using a fluorescence spectrophotometer. Figure 5a−c demonstrates how the addition of DNA with base pairs ranging from 0 to 7.0 × 10^{-5} M altered the fluorescence spectra of [H$_2$TMPyP]$^{4+}$, [Co(II)TMPyP]$^{4+}$, and [Zn(II)-TMPyP]$^{4+}$, respectively. As shown in Figure 5a, the free base porphyrin exhibited a peak centered at ∼658 nm with a hump at about 710 nm and then changed the spectral pattern from a single peak to two peaks upon the addition of DNA. The intensity of the peak appearing at 656 nm decreases, and a new peak appears at approximately 626 nm upon the addition of DNA. At a high concentration of DNA, for example, 7.0 × 10^{-4} M base pairs, the peak appearing at 626 nm exhibited its highest intensity. The spectral change of the free base porphyrin upon the addition of DNA is indicating the interactions of DNA with the porphyrin. Similar fluorescence spectrum changes of the free base porphyrin with the addition of DNA have been observed in our earlier investigations.[18,20,22]

On the other hand, both the metalloporphyrins, [Co(II)-TMPyP]$^{4+}$ and [Zn(II)TMPyP]$^{4+}$, exhibited a single peak that appeared at approximately 628 nm, and the intensity decreases with the addition of DNA ranging from 0 to 7.0 × 10^{-5} M base pairs (Figure 5a,b). The results indicate that the peak intensity is decreased because of the interaction between the free base porphyrin and its metalloderivatives with DNA. It is noted that the peak intensity decreased upon the addition of a small amount of DNA and then increased with further addition of DNA. It is noted that the presence of aggregated form of the relevant porphyrins in the aqueous solution is responsible for the decrease in peak intensity with the addition of a small amount of DNA, followed by an increase.[18,20,22] However, the results reveal that the porphyrins are present in deaggregated form under the present experimental conditions. This is due to the interaction between the porphyrin molecules and DNA, which reduces the concentration of porphyrin. Following the
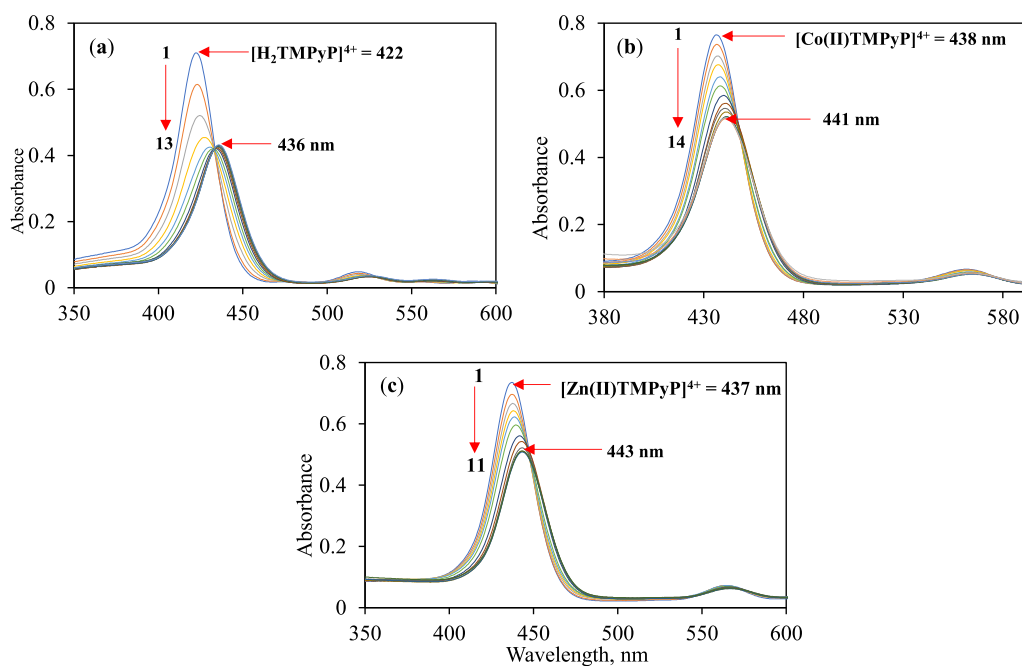
Figure 4. Change in the UV−visible spectra of (a) $[H_2TMPyP]^{4+}$ in the presence of DNA ranging from 0 to 2.0×10^{-5} M base pairs, and (b) $[Co(II)TMPyP]^{4+}$ and (c) $[Zn(II)TMPyP]^{4+}$ in the presence of DNA within a range from 0 to 2.4×10^{-4} M base pairs. The total concentration of both the free base porphyrin and metalloporphyrins is 3.6×10^{-6} M. Cell path length is 10 mm. Solution pH: 7.40 (0.02 M HEPES).
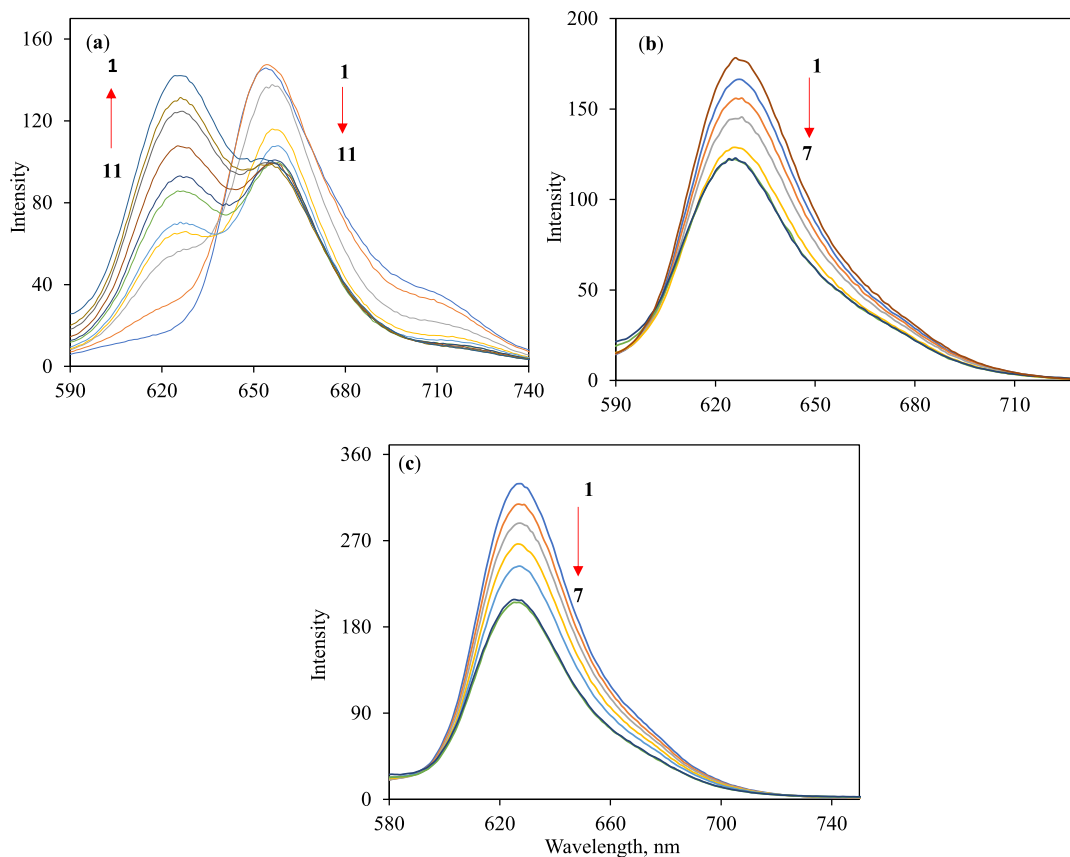
Figure 5. Change in fluorescence spectra of (a) $[H_2TMPyP]^{4+}$ in the presence of DNA ranging from 0 to 2.0×10^{-5} M base pairs, and (b) $[Co(II)TMPyP]^{4+}$ and (c) $[Zn(II)TMPyP]^{4+}$ in the presence of DNA within a range from 0 to 2.4×10^{-4} M base pairs. The total concentration of both the free base porphyrin and metalloporphyrins is 3.6×10^{-6} M. Solution pH: 7.40 (0.02 M HEPES).

addition of a large amount of DNA, the peak intensity remained constant, indicating that the formation of DNA-porphyrin adducts had been completed.[18,20,22] Initially, the cationic metalloporphyrin molecules including [Co(II)-
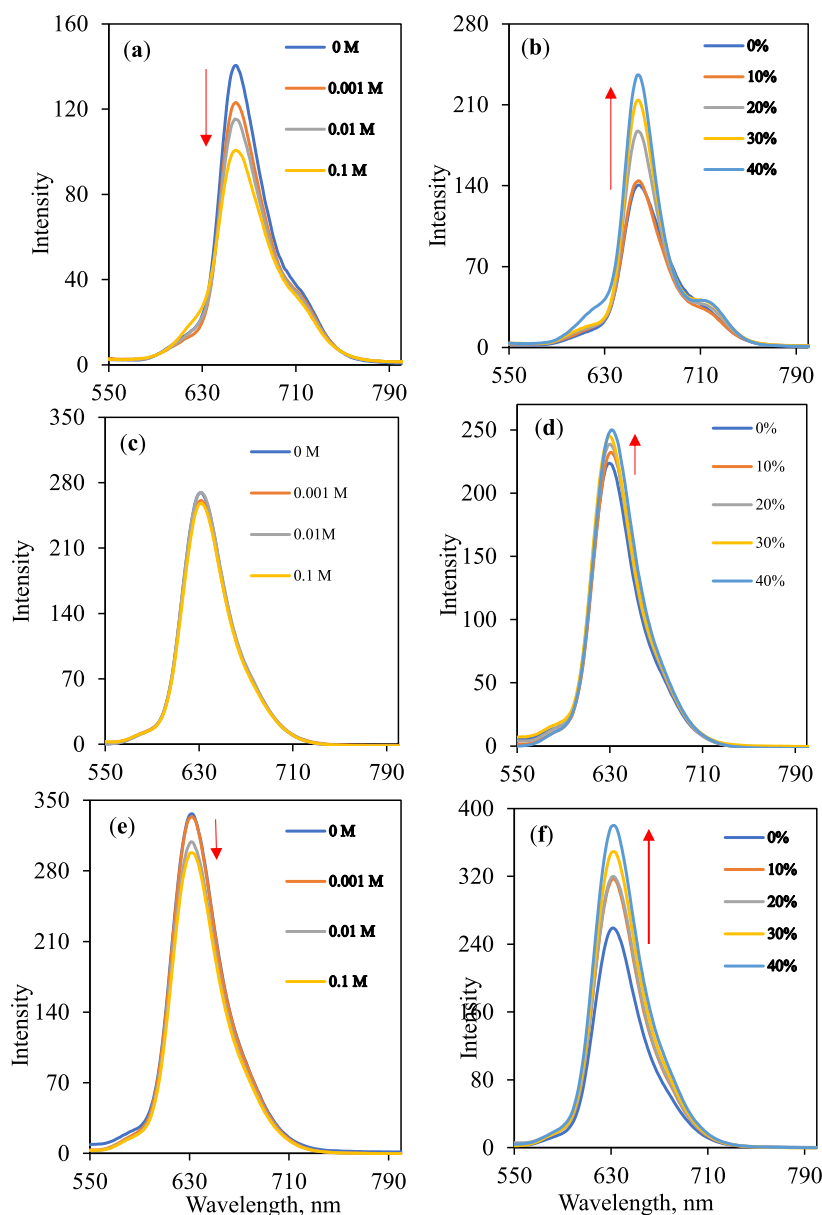
Figure 6. Fluorescence spectra of $[H_2TMPyP]^{4+}$, $[Co(II)TMPyP]^{4+}$, and $[Zn(II)TMPyP]^{4+}$ in the presence NaCl (0−0.1 M) (a) and ethanol (0−40%) (b), NaCl (0−0.1 M) (c) and ethanol (0−40%) (d), NaCl (0−0.1 M) (e), and ethanol (0−40%) (f), respectively. Solution pH: 7.40 (0.02 M HEPES). The total concentrations of both the free base porphyrin and metalloporphyrins are 3.6×10^{-6} M. Cell path length is 10 mm.

$TMPyP]^{4+}$ and $[Zn(II)TMPyP]^{4+}$ start to self-stack (aggregated) on the phosphate network of DNA and then deaggregate and interact with DNA through outside self-stacking along with partial intercalation.[18,20,22]

The aggregated and deaggregated forms of the free base porphyrin and the metalloporphyrins have been confirmed through monitoring the changes of peak intensities of the porphyrins upon addition of various concentrations of NaCl and ethanol to the porphyrin solution in the absence of DNA.[18,20,22] As can be shown in Figure 6a, the peak intensity at 658 nm reduces with increasing NaCl concentration, ranging from 0 to 0.1 M. According to this result, the free base porphyrin originally exists in a deaggregated form; however, the addition of NaCl solution leads to the porphyrin molecules to aggregate. The ions, in particular $Cl^-_{(aq)}$ ions, gather close to the tetracationic porphyrin's positive charge, which lowers the Coulombic force of repulsion.[18,20,22] However, the addition of

ethanol shows enhanced intensity of the emission spectra (Figure 6b). This demonstrates that when the concentration of ethanol increased, the aggregate form of the free base porphyrin was destroyed, resulting in the development of the monomer bands and an increase in the fluorescence intensities.

These results thus confirm that the free base porphyrin intercalated into the DNA bases in the presence of extra DNA, progressively changing from the aggregate to the monomer form and increasing the fluorescence intensity.[18,20,22]

When a range of concentrations (0−0.1 M) of NaCl were added without DNA, the fluorescence spectra of the $[Co(II)TMPyP]^{4+}$ remained unchanged (Figure 6c); however, when the concentration of ethanol increased (Figure 6d), they increased.

These results confirm that initially $[Co(II)TMPyP]^{4+}$ exists as an aggregate form in the absence of DNA but addition of ethanol deaggregates, resulting in increasing the spectral

Table 1. Antibacterial Activity of [Co(II)TMPyP]⁴⁺ and [Zn(II)TMPyP]⁴⁺ Compared to the Standard

bacteria and fungi sample	standard (ciprofloxacin)	[Co(II)TMPyP]⁴⁺	[Zn(II)TMPyP]⁴⁺	Co(II) ion	Zn(II) ion	free base porphyrin
Bacillus sereus (+)	25					
Bacillus megaterium (+)	20	14	11			
B. subtilis (+)	25	9				
S. aureus (+)	25					
Sarcina lutea (+)	20		7			
S. paratyphi (−)	25	11	10			
S. typhi (−)	26	16	8			
V. parahemolyticus (−)	25					
E. coli (−)	24		9			
V. mimicus (−)	25	12	10			
S. dysenteriae (−)	30					
Pseudomonas aureus (−)	25					
S. boydii (−)	25					
A. niger (fungi)	25	12	10			
C. albicans (fungi)	23	9	10			
S. cerevisiae (fungi)	20	10				

Scheme 1. Proposed Mechanism of the Antimicrobial Activity of Co(II)- and [Zn(II)TMPyP]⁴⁺ Complexes
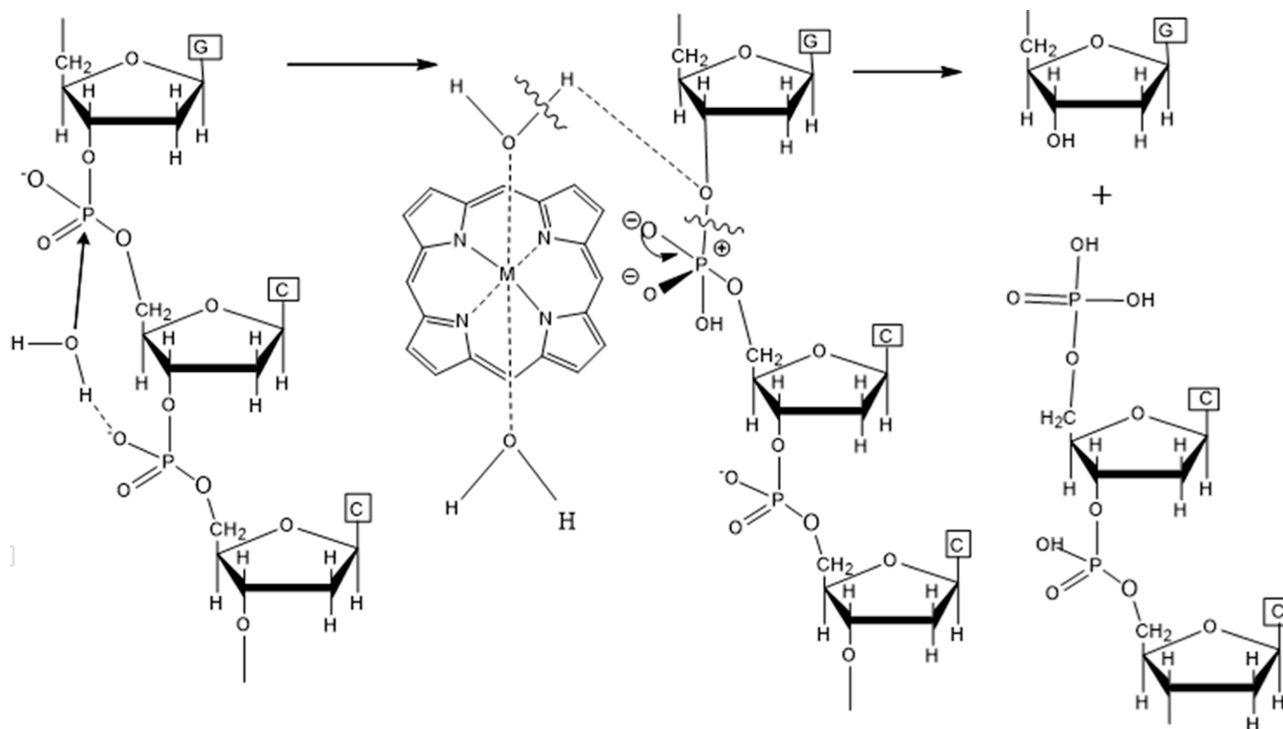
intensity. It is therefore concluded that the addition of DNA deaggregates the [Co(II)TMPyP]⁴⁺, and the monomer form interacts with DNA.[18,20,22]

In contrast to free base porphyrin, it was found that adding NaCl from 0 to 0.1 M without adding DNA decreased the intensity of the fluorescence spectra of [Zn(II)TMPyP]⁴⁺ at 628 nm. These findings imply that the presence of NaCl causes cationic porphyrin molecules to aggregate. By the formation of an anionic layer close to the cationic pyridinium moieties, the presence of chloride (Cl⁻) ions lowers the positive charge of the cationic porphyrins. This decreases the force of repulsive force, which leads to aggregation (Figure 6e). On the other hand, the intensity of the emission spectra of [Zn(II)-TMPyP]⁴⁺ increases with increasing the concentration of ethanol (Figure 6f). These results suggest that initially [Zn(II)TMPyP]⁴⁺ was present in a partially aggregated form.

The addition of NaCl reduces the positive charge of [Zn(II)TMPyP]⁴⁺, resulting in a reduction in the Coulombic force of repulsion. This is the reason for aggregation of [Zn(II)TMPyP]⁴⁺ upon the addition of NaCl. But the ethanol addition shows the enhancement in the intensity of the emission spectra. These findings show that when ethanol concentrations increased, the aggregation form of [Zn(III)-TMPyP]⁴⁺ was destroyed, resulting in the formation of monomer bands and an increase in their fluorescence intensities. It is therefore concluded that the addition of DNA deaggregates [Zn(II)TMPyP]⁴⁺, and the monomer form interacts with DNA.[18,20,22]

3.3. Antimicrobial Activity. One of the objectives of this study was to formulate new metallocomplexes based on porphyrins that may inhibit sporadic bacteria without causing any harm, in contrast to known antibiotics. With this aim,

$[Co(II)TMPyP]^{4+}$ and $[Zn(II)TMPyP]^{4+}$ were screened in vitro for their antimicrobial activities against both Gram-positive and Gram-negative bacterial strains as well as pathogenic fungi (filamentous) using disc diffusion method.[65] Blank run of counter metal ions and free base porphyrin helped us to find out if they show any antimicrobial activity at that concentration level. The diameter of the zone of inhibition in millimeters was used to evaluate the antibacterial activity of the metalloporphyrins. The findings of this study are summarized in Table 1.

The results show that $[Co(II)TMPyP]^{4+}$ inhibited two, while $[Zn(II)TMPyP]^{4+}$ inhibited only one out of five Gram-positive bacteria. $[Co(II)TMPyP]^{4+}$ and $[Zn(II)TMPyP]^{4+}$ inhibited three and four of eight Gram-negative bacteria, respectively. On the other hand, $[Co(II)TMPyP]^{4+}$ showed a 100% inhibitory effect on fungi, whereas $[Zn(II)TMPyP]^{4+}$ only exhibited a roughly 67% inhibition. At comparable metalloporphyrin concentrations, however, neither the counter metal ions nor the free base porphyrin had any antibacterial activity.

It is noted that the free base porphyrin and its metalloderivatives such as $[Co(II)TMPyP]^{4+}$ and $[Zn(II)TMPyP]^{4+}$ interact with DNA. It has been reported that the antibiotic, ciprofloxacin, interacts with bacterial DNA gyrase and thus prevents the growth of microbes. Probably, the hydroxyl part of carboxylic acid group of ciprofloxacin forms hydrogen bonding with the phosphodiester bonds and cleave the phosphodiester bonds leaving the free $5'$ phosphate and $3'$ hydroxyl groups. Furthermore, the mechanism of restriction enzyme-catalyzed DNA cleavage is identical to that of antibiotics.

The axial water molecules in the metallocomplexes undergo activation as nucleophiles and participate in the in-line displacement reaction that cleaves DNA molecules at the 3 positions.[66] Herein, metalloporphyrins with water as an axial ligand also function as cofactors in the DNA cleavage process. In the present case, the phosphodiester bond hydrolysis process resembles the substrate-assisted catalysis hypothesis that is widely suggested for all restriction endonucleases.[67] Because the cationic metal ion in the metalloporphyrins functions as a Lewis acid, it withdraws electrons from water molecules at their axial position. As a result, the proton of the water molecules becomes free, forms an attack nucleophile link with the oxygen atom on the nearby guanine base, and cleaves the phosphodiester bond to produce $3'$ −OH and $5'$ -phosphate ends. It is noteworthy to mention that the lack of an axial ligand prevented free base porphyrin from cleaving DNA. The proposed mechanism by which axial ligands containing metalloporphyrins exhibit antibacterial activity is depicted in Scheme 1.

Metallic nanoparticles, in particular silver nanoparticles (Ag-NPs), have also been studied as antibacterial agents as an alternative to conventional chemical compounds.[68−71] The results demonstrated remarkable antibacterial efficacy against various clinically isolated bacteria and fungi. The mode of action of Ag-NPs against microorganisms is still not fully understood. Nonetheless, a number of assumptions have been put out to account for the antimicrobial activities of Ag-NPs: (i) generation of reactive oxygen species; (ii) release of Ag^+ ions from Ag-NPs, which denature proteins through the formation of bonds with sulfhydryl groups; and (iii) attachment of Ag-NPs on microbes, resulting in damaging the bacteria as well as fungi.[72−74]

4. CONCLUSIONS

Thus, it may be concluded that the metalloporphyrins, such as $[Co(II)TMPyP]^{4+}$ and $[Zn(II)TMPyP]^{4+}$, interact with DNA via outside self-stacking with partial intercalation, whereas the free base porphyrin, $[H_2TMPyP]^{4+}$, interacts with DNA through intercalation. Results from fluorescence spectroscopy further confirm that the free base porphyrin and its metalloderivatives, $[Co(II)TMPyP]^{4+}$ and $[Zn(II)TMPyP]^{4+}$, interact with DNA. The free base porphyrin's emission peak splits into two; however, the metalloporphyrins only displayed a declining trend when further DNA was added, indicating that the two types of porphyrins interact differently in terms of their axial ligands. The antibacterial activities of metalloporphyrins raise the possibility of developing novel, nontoxic, and nonincursive antimicrobial strategies based on porphyrins that are more effective and faster than the current generation of antibiotics. In the future, metalloporphyrins, in particular, Zn(II)porphyrins and other medicinally valuable metals like Pt(II)-, Au(III)porphyrins, etc., may be employed for the development of novel antimicrobial and/or emergency diseases like COVID-19 drugs.

■ AUTHOR INFORMATION

Corresponding Author

Ahsan Habib − Department of Chemistry, University of Dhaka, Dhaka 1000, Bangladesh; ◉ orcid.org/0000-0001-6378-5915; Email: habibchem@du.ac.bd

Authors

Nusrat Jahan Upoma − Department of Chemistry, University of Dhaka, Dhaka 1000, Bangladesh

Nazmin Akter − Department of Chemistry, University of Dhaka, Dhaka 1000, Bangladesh

Farhana Khanam Ferdousi − Department of Chemistry, University of Dhaka, Dhaka 1000, Bangladesh

Md. Zakir Sultan − Centre for Advanced Research in Sciences (CARS), University of Dhaka, Dhaka 1000, Bangladesh

Shofiur Rahman − Biological and Environmental Sensing Research Unit, King Abdullah Institute for Nanotechnology, King Saud University, Riyadh 11451, Saudi Arabia; ◉ orcid.org/0000-0003-4219-4758

Abdullah Alodhayb − Biological and Environmental Sensing Research Unit, King Abdullah Institute for Nanotechnology, King Saud University, Riyadh 11451, Saudi Arabia; ◉ orcid.org/0000-0003-0202-8712

Khuloud A. Alibrahim − Department of Chemistry, College of Science, Princess Nourah Bint Abdulrahman University, Riyadh 11671, Saudi Arabia

Complete contact information is available at:
https://pubs.acs.org/10.1021/acsomega.4c01708

Notes

The authors declare no competing financial interest.

■ REFERENCES

(1) Santoro, A. M.; Lo Giudice, M. C.; D'Urso, A.; Lauceri, R.; Purrello, R.; Milardi, D. Cationic porphyrins are reversible proteasome inhibitors. *J. Am. Chem. Soc.* **2012**, *134*, 10451−10457.

(2) Valicsek, Z.; Horváth, O. Application of the electronic spectra of porphyrins for analytical purposes: The effects of metal ions and structural distortions. *Microchem. J.* **2013**, *107*, 47−62.

(3) Valicsek, Z.; Eller, G.; Horváth, O. Equilibrium, photophysical and photochemical examination of anionic lanthanum (III) mono-and bisporphyrins: the effects of the out-of-plane structure. *Dalton Trans.* **2012**, *41*, 13120−13131.

(4) Valicsek, Z.; Horváth, O.; Lendvay, G.; Kikaš, I.; Škorić, I. Formation, photophysics, and photochemistry of cadmium (II) complexes with 5, 10, 15, 20-tetrakis (4-sulfonatophenyl) porphyrin and its octabromo derivative: The effects of bromination and the axial hydroxo ligand. *J. Photochem. Photobiol., A* **2011**, *218*, 143−155.

(5) Ptaszyńska, A. A.; Trytek, M.; Borsuk, G.; Buczek, K.; Rybicka-Jasińska, K.; Gryko, D. Porphyrins inactivate Nosema spp. Microsporidia. *Sci. Rep.* **2018**, *8*, 5523.

(6) Rapozzi, V.; Juarranz, A.; Habib, A.; Ihan, A.; Strgar, R. Is haem the real target of COVID-19? *Photodiagn. Photodyn. Ther.* **2021**, *35*, 102381.

(7) Varchi, G.; Foglietta, F.; Canaparo, R.; Ballestri, M.; Arena, F.; Sotgiu, G.; Guerrini, A.; Nanni, C.; Cicoria, G.; Cravotto, G.; Fanti, S.; et al. Engineered porphyrin loaded core-shell nanoparticles for selective sonodynamic anticancer treatment. *Nanomedicine* **2015**, *10*, 3483−3494.

(8) Zucca, P.; Neves, C. M.; Simões, M.; Neves, M. D.; Cocco, G.; Sanjust, E. Immobilized lignin peroxidase-like metalloporphyrins as reusable catalysts in oxidative bleaching of industrial dyes. *Molecules* **2016**, *21*, 964.

(9) Biesaga, M. Porphyrins in analytical chemistry. A review. *Talanta* **2000**, *51*, 209−224.

(10) Leng, F.; Liu, H.; Ding, M.; Lin, Q. P.; Jiang, H. L. Boosting photocatalytic hydrogen production of porphyrinic MOFs: the metal location in metalloporphyrin matters. *ACS Catal.* **2018**, *8*, 4583−4590.

(11) Dini, D.; Calvete, M. J.; Hanack, M. Nonlinear optical materials for the smart filtering of optical radiation. *Chem. Rev.* **2016**, *116*, 13043−13233.

(12) de la Torre, G.; Bottari, G.; Sekita, M.; Hausmann, A.; Guldi, D. M.; Torres, T. A voyage into the synthesis and photophysics of homo-and heterobinuclear ensembles of phthalocyanines and porphyrins. *Chem. Soc. Rev.* **2013**, *42*, 8049−8105.

(13) Saito, S.; Osuka, A. Expanded porphyrins: intriguing structures, electronic properties, and reactivities. *Angew. Chem., Int. Ed.* **2011**, *50*, 4342−4373.

(14) Hambright, R.; Kadish, K. M.; Smith, K. M.; Guilard, R. The Porphyrin Handbook. In *Chemistry of Water Soluble Porphyrins*, Kadish, K. M., Smith, K. M., Guilard, R., Eds.; Academic Press: New York, 2000; p 129.

(15) Habib, A.; Tabata, M.; Wu, Y. G. Kinetics and mechanism of gold (III) incorporation into tetrakis (1-methylpyridium-4-yl) porphyrin in aqueous solution. *J. Porphyrins Phthalocyanines* **2004**, *08*, 1269−1275.

(16) Pasternack, R. F.; Gibbs, E. J.; Villafranca, J. J. Interactions of porphyrins with nucleic acids. *Biochemistry* **1983**, *22*, 2406−2414.

(17) Pasternack, R. F.; Gibbs, E. J.; Villafranca, J. J. Interactions of porphyrins with nucleic acids. *Biochemistry* **1983**, *22*, 5409−5417.

(18) Nyarko, E.; Hanada, N.; Habib, A.; Tabata, M. Fluorescence and phosphorescence spectra of Au (III), Pt (II) and Pd (II) porphyrins with DNA at room temperature. *Inorg. Chim. Acta* **2004**, *357*, 739−745.

(19) Nyarko, E.; Hara, T.; Grab, D. J.; Habib, A.; Kim, Y.; Nikolskaia, O.; Fukuma, T.; Tabata, M. In vitro toxicity of palladium (II) and gold (III) porphyrins and their aqueous metal ion counterparts on Trypanosoma brucei brucei growth. *Chem. Biol. Interact.* **2004**, *148*, 19−25.

(20) Habib, M. A.; Sarker, A. K.; Tabata, M. Interactions of DNA with H2TMPyP4+ and Ru(II)TMPyP4+: Probable Lead Compounds for African Sleeping Sickness. *Bangladesh Pharm. J.* **2015**, *17*, 79−85.

(21) Habib, A.; Islam, R.; Chakraborty, M.; Serniabad, S.; Khan, M. S.; Qais, D. S.; Quayum, M. E.; Alam, M. A.; Ismail, I.; Tabata, M. Kinetics and mechanism of incorporation of zinc (II) into tetrakis (1-methylpyridium-4-yl) porphyrin in aqueous solution. *Arabian J. Chem.* **2020**, *13*, 6552−6558.

(22) Habib, A.; Serniabad, S.; Khan, M. S.; Islam, R.; Chakraborty, M.; Nargis, A.; Quayum, M. E.; Alam, M. A.; Rapozzi, V.; Tabata, M. Kinetics and mechanism of formation of nickel (II) porphyrin and its interaction with DNA in aqueous medium. *J. Chem. Sci.* **2021**, *133*, 83.

(23) Pasternack, R. F.; Gibbs, E. J. *Metal Ions in Biological Systems.* Marcel Dekker Inc., New York, 1997, Vol. 33; p 367−397.

(24) Pratviel, G.; Bernadou, J.; Meunier, B. *Metal Ions in Biological Systems.* Marcel Dekker Inc., New York, 1997, Vol. 33; p 399−426.

(25) Pasternack, R. F.; Gibbs, E. J. *Semin. Hematol.* **1989**, *26*, 77.

(26) Banville, D. L.; Marzilli, L. G.; Strickland, J. A.; Wilson, W. D. Comparison of the effects of cationic porphyrins on DNA properties: influence of GC content of native and synthetic polymers. *Biopolymers* **1986**, *25*, 1837−1858.

(27) Ford, K.; Fox, K. R.; Neidle, S.; Waring, M. J. DNA sequence preferences for an intercalating porphyin compound revealed by footprinting. *Nucleic Acids Res.* **1987**, *15*, 2221−2234.

(28) Ward, B.; Skorobogaty, A.; Dabrowiak, J. C. DNA binding specificity of a series of cationic metalloporphyrin complexes. *Biochemistry* **1986**, *25*, 7827−7833.

(29) Gibbs, E. J.; Tinoco, I.; Maestre, M. F.; Ellinas, P. A.; Pasternack, R. F. Self-assembly of porphyrins on nucleic acid templates. *Biochem. Biophys. Res. Commun.* **1988**, *157*, 350−358.

(30) Almeida, A.; Cunha, A.; Faustino, M. A.; Tomé, A. C.; Neves, M. G. Porphyrins as antimicrobial photosensitizing agents. In *Photodynamic inactivation of microbial pathogens: Medical and Environmental Applications*; RSC Publishing: Cambridge, UK, 2011; pp 83−160.

(31) Maisch, T.; Hackbarth, S.; Regensburger, J.; Felgenträger, A.; Bäumler, W.; Landthaler, M.; Röder, B. Photodynamic inactivation of multi-resistant bacteria (PIB)-a new approach to treat superficial infections in the 21st century. *J. Dtsch. Dermatologischen Ges.* **2011**, *9*, 360−366.

(32) Felifel, N. T.; Sliem, M. A.; Kamel, Z.; Bojarska, J.; Seadawy, M. G.; Amin, R. M.; Elnagdy, S. M. Antimicrobial Photodynamic Therapy against Escherichia coli and Staphylococcus aureus Using Nanoemulsion-Encapsulated Zinc Phthalocyanine. *Microorganisms* **2023**, *11*, 1143.

(33) Carrel, M.; Perencevich, E. N.; David, M. Z. USA300 methicillin-resistant Staphylococcus aureus, United States, 2000−2013. *Emerging Infect. Dis.* **2015**, *21*, 1973−1980.

(34) Harada, N.; Togashi, A.; Aung, M. S.; Kunizaki, J.; Nogami, K.; Nagaoka, Y.; Ishii, A.; Kosukegawa, I.; Aisaka, W.; Nakamura, S.; Wakabayashi, T.; Tsugawa, T.; Kobayashi, N. Acute osteomyelitis/septic pulmonary embolism associated with familial infections caused by PVL-positive ST6562 MRSA-IVa, a presumptive variant of USA300 clone. *IJID Reg.* **2023**, *8*, 16−18.

(35) Pollack, A. Rising Threat of Infections Unfazed by Antibiotics. 2018. New York Times, http://www.biocence.com/download/raging_antibiotic.pdf.

(36) Songca, S. P.; Oluwafemi, O. S. Photodynamic therapy: A new light for the developing world. *Afr. J. Biotechnol.* **2013**, *12*, 3590−3599.

(37) Amos-Tautua, B. M.; Songca, S. P.; Oluwafemi, O. S. Application of porphyrins in antibacterial photodynamic therapy. *Molecules* **2019**, *24*, 2456.

(38) Galstyan, A.; Maurya, Y. K.; Zhylitskaya, H.; Bae, Y. J.; Wu, Y.-L.; Wasielewski, M. R.; Lis, T.; Dobrindt, U.; Stępień, M. π-Extended Donor-Acceptor Porphyrins and Metalloporphyrins for Antimicrobial Photodynamic Inactivation. *Chem. Eur. J.* **2020**, *26*, 8262−8266.

(39) Wise, R.; Blaser, M.; Carrs, O.; Cassell, G.; Fishman, N.; Guidos, R.; Levy, S.; Powers, J.; Norrby, R.; Tillotson, G.; et al. BSAC Working Party on The Urgent Need: Regenerating Antibacterial Drug Discovery and Development. The urgent need for new antibacterial agents. *J. Antimicrob. Chemother.* **2011**, *66*, 1939−1940.

(40) Cotter, P. D.; Ross, R. P.; Hill, C. Bacteriocins - a viable alternative to antibiotics? *Nat. Rev. Microbiol.* **2013**, *11*, 95−105.

(41) Tegos, G. P.; Hamblin, M. R. Disruptive innovations, new anti-infectives in the age of resistance. *Curr. Opin. Pharmacol.* **2013**, *13*, 673−677.

(42) Hamblin, M. Antimicrobial photodynamic inactivation: A bright new technique to kill resistant microbes. *Curr. Opin. Microbiol.* **2016**, *33*, 67−73.

(43) Chitsazi, M. T.; Shirmohammadi, A.; Pourabbas, R.; Abolfazli, N.; Farhoudi, I.; Azar, B. D.; Farhadi, F. Clinical and microbiological effects of photodynamic therapy associated with non-surgical treatment in aggressive periodontitis. *J. Dental Res. Dental Clin. Dental Prospects* **2014**, *8*, 153−159.

(44) Garcia, V. G.; de Lima, M. A.; Okamoto, T.; Milanezi, L. A.; Júnior, E. C. G.; Fernandes, L. A.; de Almeida, J. M.; Theodoro, L. H. Effect of photodynamic therapy on the healing of cutaneous third-degree-burn: histological study in rats. *Lasers Med. Sci.* **2010**, *25*, 221−228.

(45) Balderas-Rentería, I.; López-Cortina, S.; Arredondo-Espinoza, E. Synthesis and Photodynamic Activity of 5, 10, 15-Tris (p-chlorophenyl)-20-(2-hydroxy-3-methoxyphenyl)-21H, 23H-porphyrin. *J. Mex. Chem. Soc.* **2014**, *58*, 369−373.

(46) Hashimoto, M. C. E.; Prates, R. A.; Kato, I. T.; Nunez, S. C.; Courrol, L. C.; Ribeiro, M. S. Antimicrobial photodynamic therapy on drug-resistant Pseudomonas aeruginosa-induced infection. An in vivo study. *Photochem. Photobiol.* **2012**, *88*, 590−595.

(47) Tabata, M.; Nakajima, K.; Nyarko, E. Metalloporphyrin mediated DNA cleavage by a low concentration of HaeIII restriction enzyme. *J. Inorg. Biochem.* **2000**, *78*, 383−389.

(48) Tabata, M.; Kumar Sarker, A.; Nyarko, E. Enhanced conformational changes in DNA in the presence of mercury(II), cadmium(II) and lead(II) porphyrins. *J. Inorg. Biochem.* **2003**, *94*, 50−58.

(49) Ahsan Habib, A. H.; Tatsuru Hara, T. H.; Aklima Nargis, A. N.; Nyarko, E.; Tabata, M. DNA Cleavage and Trypanosomes Death by a Combination of Alamar Blue and Au (III). *J. Chem. Soc. Pak.* **2020**, *42*, 141−148.

(50) Prasanth, C. S.; Karunakaran, S. C.; Paul, A. K.; Kussovski, V.; Mantareva, V.; Ramaiah, D.; Selvaraj, L.; Angelov, I.; Avramov, L.; Nandakumar, K.; Subhash, N. Antimicrobial photodynamic efficiency of novel cationic porphyrins towards periodontal Gram-positive and Gram-negative pathogenic bacteria. *Photochem. Photobiol.* **2014**, *90*, 628−640.

(51) Seeger, M. G.; Ries, A. S.; Gressler, L. T.; Botton, S. A.; Iglesias, B. A.; Cargnelutti, J. F. In vitro antimicrobial photodynamic therapy using tetra-cationic porphyrins against multidrug-resistant bacteria isolated from canine otitis. *Photodiagn. Photodyn. Ther.* **2020**, *32*, 101982.

(52) Pinto, S. C.; Acunha, T. V.; Santurio, J. M.; Denardi, L. B.; Iglesias, B. A. Investigation of powerful fungicidal activity of tetra-cationic platinum(II) and palladium(II) porphyrins by antimicrobial photodynamic therapy assays. *Photodiagn. Photodyn. Ther.* **2021**, *36*, 102550.

(53) da Silva Canielles Caprara, C.; da Silva Freitas, L.; Iglesias, B. A.; Ferreira, L. B.; Ramos, D. F. Charge effect of water-soluble porphyrin derivatives as a prototype to fight infections caused by

Acinetobacter baumannii by aPDT approaches. *Biofouling* **2022**, *38*, 605−613.

(54) Batishchev, O. V.; Kalutskii, M. A.; Varlamova, E. A.; Konstantinova, A. N.; Makrinsky, K. I.; Ermakov, Y. A.; Meshkov, I. N.; Sokolov, V. S.; Gorbunova, Y. G. Antimicrobial activity of photosensitizers: arrangement in bacterial membrane matters. *Front. Mol. Biosci.* **2023**, *10*, 1192794.

(55) Makino, T.; Itoh, J. *J. Clin. Chem.* **1979**, *8*, 296.

(56) Eugster, N.; Fermín, D. J.; Girault, H. H. Photoinduced electron transfer at liquid|liquid interfaces: dynamics of the heterogeneous photoreduction of quinones by self-assembled porphyrin ion pairs. *J. Am. Chem. Soc.* **2003**, *125*, 4862−4869.

(57) Larsen, R. W.; Miksovska, J.; Musselman, R. L.; Wojtas, L. Ground- and excited-state properties of Zn(II) tetrakis(4-tetramethylpyridyl) pophyrin specifically encapsulated within a Zn(II) HKUST metal-organic framework. *J. Phys. Chem. A* **2011**, *115*, 11519−11524.

(58) de Sousa Neto, D.; Hawe, A.; Tabak, M. Interaction of meso-tetrakis (4-N-methylpyridyl) porphyrin in its free base and as a Zn(II) derivative with large unilamellar phospholipid vesicles. *Eur. Biophys. J.* **2013**, *42*, 267−279.

(59) Benz, O. S.; Yuan, Q.; Cronican, A. A.; Peterson, J.; Pearce, L. L. Effect of Ascorbate on the Cyanide-Scavenging Capability of Cobalt(III) meso-Tetra(4-N-methylpyridyl)porphine Pentaiodide: Deactivation by Reduction? *Chem. Res. Toxicol.* **2016**, *29*, 270−278.

(60) Hambright, P. *The Porphyrin Handbook*, Kadish, K. M., Smith, K. M. R., Guilard, R., Eds.; Academic Press: San Diego, 2002; p 163.

(61) Carvlin, M. J.; Fiel, R. J. Intercalative and nonintercalative binding of large cationic porphyrin ligands to calf thymus DNA. *Nucleic Acids Res.* **1983**, *11*, 6121−6139.

(62) Carvlin, M. J.; Mark, E.; Fiel, R.; Howard, J. C. Intercalative and nonintercalative binding of large cationic porphyrin ligands to polynucleotides. *Nucleic Acids Res.* **1983**, *11*, 6141−6154.

(63) Dougherty, G. Intercalation of tetracationic metalloporphyrins and related compounds into DNA. *J. Inorg. Biochem.* **1988**, *34*, 95−103.

(64) Guliaev, A. B.; Leontis, N. B. Cationic 5,10,15,20-tetrakis(N-methylpyridinium-4-yl)porphyrin fully intercalates at 5′-CG-3′ steps of duplex DNA in solution. *Biochemistry* **1999**, *38*, 15425−15437.

(65) Bauer, A. W.; Kirby, W. M. M.; Sherris, J. C.; Turck, M. Antibiotic Susceptibility Testing by a Standardized Single Disk Method. *Am. J. Clin. Pathol.* **1966**, *45*, 493−496.

(66) Jeltsch, A.; Alves, J.; Wolfes, H.; Maass, G.; Pingoud, A. Substrate-assisted catalysis in the cleavage of DNA by the EcoRI and EcoRV restriction enzymes. *Proc. Natl. Acad. Sci. U S A* **1993**, *90*, 8499−8503.

(67) Aiken, C. R.; Fisher, E. W.; Gumport, R. I. The specific binding, bending, and unwinding of DNA by RsrI endonuclease, an isoschizomer of EcoRI endonuclease. *J. Biol. Chem.* **1991**, *266*, 19063−19069.

(68) Bruna, T.; Maldonado-Bravo, F.; Jara, P.; Caro, N. Silver Nanoparticles and Their Antibacterial Applications. *Int. J. Mol. Sci.* **2021**, *22*, 7202.

(69) Muraro, P. C. L.; Pinheiro, L. D. S. M.; Chuy, G.; Vizzotto, B. S.; Pavoski, G.; Espinosa, D. C. R.; Rech, V. C.; da Silva, W. L. Silver nanoparticles from residual biomass: Biosynthesis, characterization and antimicrobial activity. *J. Biotechnol.* **2022**, *343*, 47−51.

(70) Yin, I. X.; Zhang, J.; Zhao, I. S.; Mei, M. L.; Li, Q.; Chu, C. H. The antibacterial mechanism of silver nanoparticles and its application in dentistry. *Int. J. Nanomed.* **2020**, *Volume 15*, 2555−2562.

(71) Urnukhsaikhan, E.; Bold, B. E.; Gunbileg, A.; Sukhbaatar, N.; Mishig-Ochir, T. Antibacterial activity and characteristics of silver nanoparticles biosynthesized from Carduus crispus. *Sci. Rep.* **2021**, *11*, 21047.

(72) Banala, R. R.; Nagati, V. B.; Karnati, P. R. Green synthesis and characterization of Carica papaya leaf extract coated silver nano-particles through X-ray diffraction, electron microscopy and evaluation of bactericidal properties. *Saudi J. Biol. Sci.* **2015**, *22*, 637−644.

(73) Jyoti, K.; Baunthiyal, M.; Singh, A. Characterization of silver nanoparticles synthesized using Urtica dioica Linn. Leaves and their synergistic effects with antibiotics. *J. Radiat. Res. Appl. Sci.* **2016**, *9*, 217−227.

(74) Siddiqi, K. S.; Husen, A.; Rao, R. A. K. A review on biosynthesis of silver nanoparticles and their biocidal properties. *J. Nanobiotechnol.* **2018**, *16*, 14.